2014

Small-Scale and Oil-Free Turbocompressor for Refrigeration Applications

Jürg Schiffmann
Ecole Polytechnique Federale de Lausanne, Switzerland, jurg.schiffmann@epfl.ch

Small-Scale and Oil-Free Turbocompressor for Refrigeration Applications

Jürg SCHIFFMANN

Laboratory for Applied Mechanical Design, Ecole Polytechnique Fédérale de Lausanne
Rue de la Maladière 71b, CH-2002 Neuchâtel, Switzerland
Phone: +41 21 695 45 48
jurg.schiffmann@epfl.ch

ABSTRACT

The evolution of the coefficient of performance of domestic heat pumps has been stagnating since the introduction of scroll compressors in the early nineties. Compact oil-free direct driven radial compressors represent a promising alternative to the current state of the art refrigeration compressors. The operation characteristics of dynamic compressors naturally fits the heat pump load and the absence of oil allows the full deployment of the potential of enhanced surface evaporators and the implementation of advanced multi-stage cycles both proven means to increase the heat pump performance.

This article presents the experimental investigation of a hermetic single-stage and direct-driven radial compressor supported on gas-lubricated bearings designed for domestic heat pump applications. The 20 mm tip diameter compressor was tested at rotor speeds of up to 210 krpm reaching pressure ratios in excess of 3.3 and measured isentropic efficiencies above 78% while processing R134a. Rigidly mounted herringbone grooved journal and spiral groove thrust bearings lubricated with vapor phase refrigerant fluid have been used to support the rotor. The electric motor is a permanent magnet machine delivering a mechanical power of up to 2 kW.

Further theoretical investigation based on the experimentally validated compressor design tool identifies tip clearance and relative surface roughness as the main drivers for losses in small-scale turbomachinery for refrigeration applications. The research therefore suggests that both system design to achieve small tip clearances and impeller manufacturing process require particular attention at small scale.

1. INTRODUCTION

The worldwide energy fraction consumed by the residential sector accounts for 35% of the total primary energy consumption, out of which 75% are used for domestic heating cooling and hot tap water production (IEA, 2007). Since heating and cooling only requires low temperature levels, renewables energy sources like low temperature environmental heat offer an interesting alternative to the widely spread fossil fuels. A comparison of technological combinations based on their primary energy consumption to deliver domestic heat clearly shows the significant advantages of heat pumps (Favrat *et al.* 2008). Additional prior work introduces further efficient combinations for tri-generation based on hybrid fuel cell cycles (SOFC-GT) combined with heat pumps (Burer *et al.*, 2003). Recent investigations also show interesting alternatives to thermally driven absorption heat pump cycles, based on an Organic Rankine Cycle directly driving a vapor compression heat pump (Demierre *et al.*, 2012).

Despite their significant potential for primary energy savings the Coefficient Of Performance of heat pumps has been stagnating over past years. Figure 1 represents the evolution of the COP of heat pumps tested at the Swiss heat pump certification center (Eschmann, 2008). In the early nineties the performance increased dramatically through

the introduction of the scroll compressor technology. The surge, however, was followed by a still ongoing period of stagnation. This evolution clearly raises the question whether and how a new step change in heat pumping could be introduced.

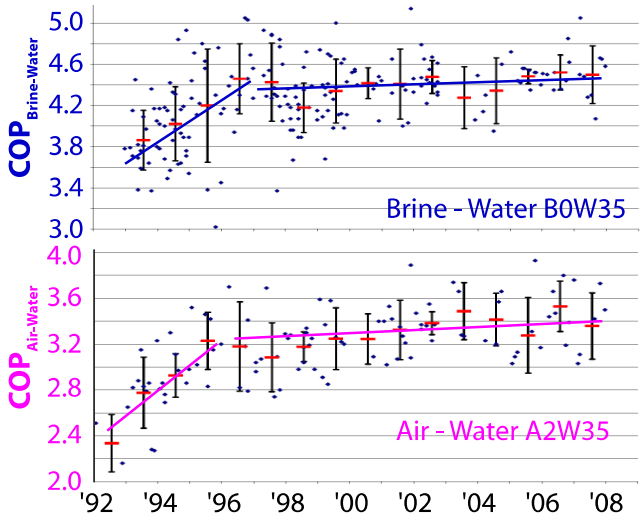

Figure 1: Evolution of the Coefficient Of Performance (COP) of heat pumps tested at the Swiss heat pump certification center (Eschmann, 2008).

Through an exergetic analysis of high temperature lift heat pumps Zehnder (2004) demonstrates that approximately 50% of the losses are generated during the compression process, whereas 20% occur in the heat exchangers. The remainder of the losses can be associated to the expansion process. One of the key enablers for decreasing the losses in the heat pump cycle is therefore to increase the compressor efficiency. This can be achieved both by improved compressor technology and by splitting the compression process into multiple stages in combination with intercooling. Further, splitting the cycle into multiple stages makes better use of the exergy of the liquid refrigerant and improves the evaporator performance. Favrat *et al.* (1997) and Zehnder (2004) have experimentally demonstrated the advantages of multi-stage domestic-scale heat pumps. Their investigation showed that the main challenge when using off-the-shelf technology is oil migration within the cycle. The oil needed for sealing and lubrication of the scroll compressors contaminates the refrigerant loop. Since no self-stabilizing configuration could be found an oil-management system had to be introduced to equilibrate the oil levels in the two compressor stages. The presence of oil in the evaporator in particular results in both increased thermal resistance and pressure losses (Youbi-Idrissi *et al.*, 2003; Zuercher *et al.*, 1998). In addition, the presence of oil is a hindrance to the deployment of the recently studied highly efficient micro-channel heat exchangers with nano-coatings.

The analysis allows to conclude that a promising way to further improve the heat pump performance is by combining multistage cycles with efficient, oil-free compressor technologies. Since dynamic machines such as radial or axial turbocompressors do not require oil for sealing or lubrication and as they are known to reach higher efficiency than volumetric machines, a single stage radial compressor has been thoroughly investigated and experimentally tested by Schiffmann and Favrat (2009, 2010a) for their introduction into domestic-scale heat pumps.

2. TEST COMPRESSOR LAYOUT

2.1. Compressor specifications

In order to investigate the technical feasibility of a small-scale turbocompressor for driving heat pumps, a single stage radial compressor supported on oil-free, dynamic gas-lubricated bearings has been designed and manufactured. The specifications for this proof-of-concept compressor correspond to the requirements of the first stage of a two

stage air-water heat pump that delivers a heat rate of 12 kW at 60°C at an external air temperature of -12°C. The corresponding thermodynamic cycle is a twin-stage heat pump cycle with an open economizer located at the intermediate pressure level. Table 1 summarizes the specifications of the compressor for five typical operation points using R134a as a working fluid. At increasing external air temperatures both the heat rate and the temperature level at which it is delivered decrease. This leads to decreasing pressure ratios and mass-flow rates. This tendency is very interesting for dynamic compressors since this evolution naturally follows the behavior of such machines. Hence, if the operational range of a particular compressor design could match all the specifications, the heat pump would not have to operate in an on-off mode but could smoothly modulate the power and the pressure ratio by simply controlling the rotor speed.

Table 1: Compressor specifications for the first stage of a twin-stage heat pump delivering a heat rate of 12 kW at 60° for an external air temperature of -12°C using R134a as a working fluid.

OP	A-12	A-7	A2	A7	A12
T_{Air} [°C]	-12	-7	2	7	12
T_{Water} [°C]	60	55	50	45	40
P_{in} [-]	0.144	0.177	0.251	0.302	0.36
Π_1 [MPa]	4.17	3.39	2.39	1.99	1.67
m_1 [kg/s]	0.053	0.043	0.024	0.016	0.005

2.2. Compressor design

The fact that the compressor stage needs to be able to operate on a wide operation range rather than on a given nominal point adds considerable complexity to the design task and to its optimization in particular. In order to achieve this task Schiffmann and Favrat (2010a) have implemented a reduced order compressor model and have linked it to a multi-objective optimizer based on evolutionary algorithms with the objective to minimize the compressor energy consumption over a complete season. The results show that the optimizer is not able to find a compressor geometry that matches all the five operation points without variable inlet guide vanes (IGV) since the mass flow specifications are too widely spread. Note that a vaneless diffuser is being used to maximize range although its efficiency is lower by to up to 3 points compared bladed diffusers. The compressor was therefore aerodynamically designed such as to best fit operation points with external air temperatures ranging from -12 to 2 °C. In this range the compressor is able to modulate the delivered power by adjusting the rotor speed. For higher air temperatures the heat pump delivers too much heat rate and will therefore have to operate in an on-off mode. Figure 2 illustrates the design variables of the complete compressor stage. Table 2 summarizes the dimensions of the tested proof-of-concept compressor stage. The detailed aerodynamic compressor design was performed by using a commercial tool. The test impeller was manufactured out of an aluminum alloy.

Table 2: Summary of the dimensions of the tested proof-of-concept compressor.

Inlet shroud radius r_{2s} [m]	0.056
Inlet hub radius r_{2s} [m]	0.001
Tip radius r_4 [m]	0.01
Diffuser exhaust radius r_5 [m]	0.0165
Tip width b_4 [m]	0.0012
Diffuser exhaust width b_5 [m]	0.001
Exhaust blade angle β_4 [deg]	-45

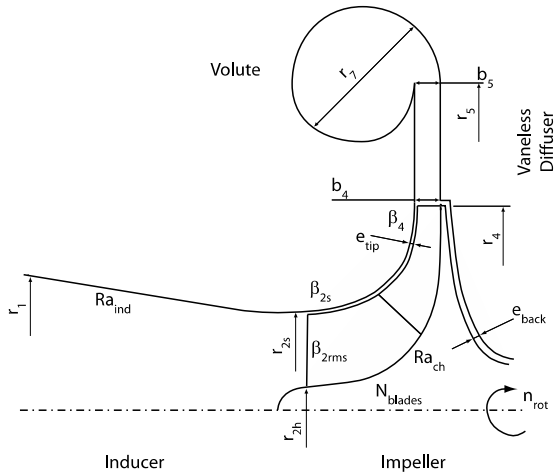

Figure 2: Design variables of the radial complete compressor stage (Schiffmann and Favrat, 2010a).

2.3. Bearing design

In order to achieve the pressure ratio for the OP A-12 the test impeller summarized in Table 2 requires rotor speeds of up to 240 krpm. This clearly leads to the question about what type of bearings to use for this application, in particular since an oil-free design is desired. Bearings are split into three classes: (1) Rolling-element bearings, (2) magnetic bearings and (3) fluid film bearings.

Rolling-element bearings require grease or oil-lubrication and yield limited lifetime, in particular at the required rotor speeds. Active magnetic bearings offer an attractive alternative since the rotor levitates in magnetic fields and yield therefore very low mechanical losses and allow wear free operation. However, these bearings require an active control which makes them expensive, moreover the rotor becomes longer and less stiff due to a stack of laminated sheets to minimize the bearing induction losses. This might limit the operation range of the turbocompressor. Fluid film bearings are further divided into externally pressurized and dynamic designs. External pressurization requires auxiliary power to produce the pressurized fluid to be injected into the fluid film. It is estimated that for the given compressor this power amounts to approximately 1 kW compared to 3 kW shaft power. Dynamic bearings generate load capacity through the rotation of the rotor itself. These latter require no auxiliary power systems and are well suited for small-scale applications since their geometry is simple and therefore easily manufacturable also at reduced scale. Fluid film bearings may be lubricated with incompressible or compressible fluids. Lubrication with a liquid phase refrigerant fluid operating close to saturation might flash within the fluid film if it is not sufficiently sub-cooled. Flashing might destabilize the rotor and therefore adds additional risks. Moreover, sealing would be required to ensure the liquid stays within the fluid film. Out of these reasons dynamic, gas-lubricated bearings have been chosen for this particular application where the lubricant is vapor phase refrigerant fluid, therefore allowing for a completely hermetic compressor unit. Herringbone grooved journal bearings and spiral grooved thrust bearings are being used. An outline of these bearings is given in Figure 3

Since the design of rotors supported on gas-lubricated bearings are likely to get dynamically unstable due to the cross-coupled nature of fluid-film bearings, the rotordynamic design of the compressor system was given considerable care. A rigid-body analysis was performed based on the spectral analysis introduced by Pan (1964) and by Lund (1968). The parametric rotordynamic tool allows to predict the whirl speed and the stability map for both conical and cylindrical rigid body modes for a given rotor and bearing geometry (Schiffmann and Favrat, 2010c). Since the bearings are lubricated with a fluid that operates close to saturation the perfect gas assumption often used when solving the Reynolds equation that governs the fluid film pressure is not valid anymore. Therefore Schiffmann and Favrat (2010b) have introduced the effect of real gas into the bearing modeling demonstrating that their effect is far from negligible.

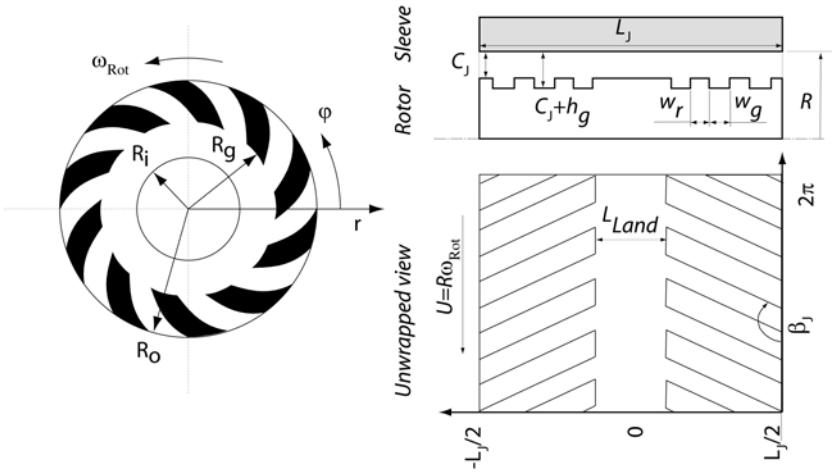

Figure 3: Herringbone groove journal and spiral groove thrust bearing geometries.

3. EXPERIMENTAL RESULTS

3.1. Compressor system

An image of the tested proof-of-concept compressor and a comparison to an equivalent scroll compressor is shown in Figure 4. The comparison clearly demonstrates the increased power density. Note that the turbocompressor is a fully hermetic and oil-free system.

Figure 4: Comparison between the proof-of-concept turbocompressor and an equivalent scroll compressor.

3.2. Test-rig setup

In order to characterize the proof-of-concept and to validate the different component models (compressor, bearing, rotordynamics) a hermetic vapor phase compressor test loop has been built and equipped with the necessary measurement equipment to characterize the single stage radial compressor. Figure 5 represents a schematic view of the closed-loop test-rig and indicates the positions of the different temperature probes, pressure transducers and mass-flow measurement. The separator, which is equipped with an electric heater avoids liquid compressor ingestion and allows to adjust the inlet superheat. Since the aerodynamic bearings operate at very low clearances a bearing aeration loop is installed to ensure clean and filtered vapor phase refrigerant fluid surrounding the bearings. The heat exchanger for extracting the compressor power is partially filled with liquid phase refrigerant to stabilize the compressor inlet conditions. The compressor inlet pressure can be adjusted by controlling the external water temperature. An external cooling loop is provided for extracting the losses from the electric motor.

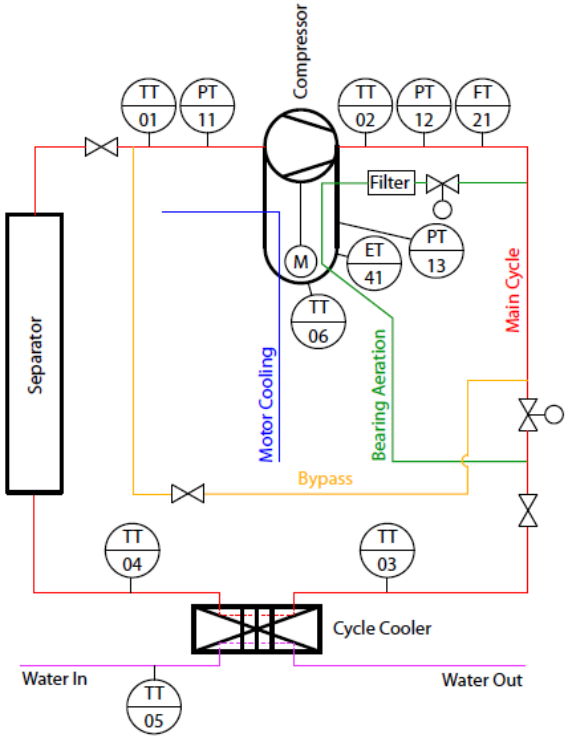

Figure 5: Representation of the vapor phase compressor test-rig indicating the main components and temperature (TT), pressure (PT), electrical power (EP), mass flow (FT) measurement locations. Further probes not indicated measure rotor speed and orbits.

3.3. Measured compressor performance

Figure 6 and Figure 7 summarize measured data collected during a test performed with compressor inlet conditions corresponding to an external air temperatures of -12°C. The experimental data is compared to the compressor performance predictions based on the 1D-compressor model developed for the preliminary aerodynamic compressor stage design. Figure 6 represents the compressor map for rotor speeds ranging from 150 to 210 krpm. At the maximum rotor speed a pressure ratio of 3.3 could be achieved, corresponding to a shaft power of 1.5 kW approximately. Unfortunately the tests had to be stopped at those rotor speeds due to too high rotor orbits resulting from shifting rotor unbalance. The full lines in the figure represent the predicted compressor map using the 1D-compresor-model. The predicted data agrees fairly well with the experimental data except for operation close to surge at high rotor speeds where the reduced order model overestimates the pressure ratio by up to 5%. Considering the highly three-dimensional nature of the flow in a radial impeller the reduced order 1D-model predicts the compressor map with sufficient accuracy. It is hypothesized that surge onset and increased inlet recirculation might be the origin of the increased discrepancy when operating the compressor close to surge.

The measured efficiencies clearly demonstrate the interesting potential of small-scale turbomachinery for refrigeration applications (heating and cooling). Remarkable efficiencies in excess of 78% are achieved even at high rotor speeds for pressure ratios in excess of 3. The efficiency prediction of the 1D-code generally underestimates the measured losses. A more thorough validation including different impeller geometries is needed to better calibrate the different implemented loss correlations.

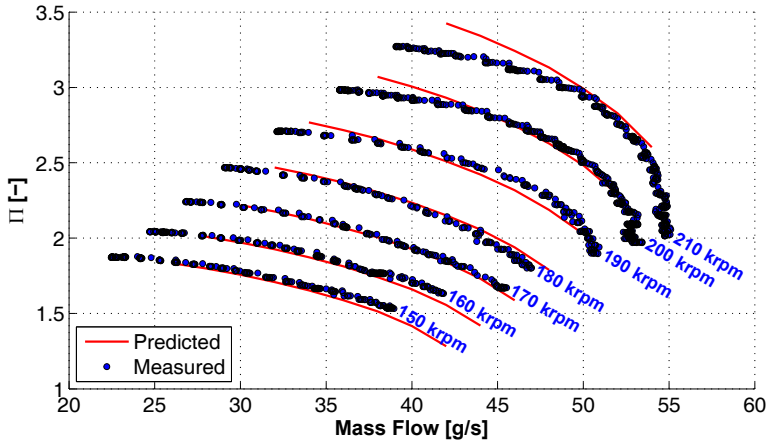

Figure 6: The measured compressor map and the 1D-model prediction for an inlet pressure of 1.44 bar corresponding to the operation point at an external air temperature of -12°C.

3.4. Analysis of performance

In order to analyze the different loss mechanisms within the compressor stage, the 1D-model has been used to identify their distribution as a function of the specific speed (ns). The different loss mechanisms are categorized into diffuser losses, internal and external impeller losses, which include the disc friction of the impeller backside and inlet recirculation. The latter increase the specific enthalpy but do not affect the pressure rise as opposed to the internal losses, which depreciate the pressure rise within the compressor.

Figure 8 represents the total loss as well as the contributions from the diffuser, internal and external losses as a function of the specific speed. The results clearly show that there is an optimum specific speed mainly driven by a trade-off between internal and external losses. The internal losses, composed of incidence, diffusion, blade loading, skin friction and clearance losses, increase with increasing rotational speed. On the other hand the external losses, disc friction and recirculation losses, increase with reduced speed (increased tip radius).

Figure 9 shows the relative split between (1) internal, external and diffuser losses, (2) the internal losses (sf: skin friction, bl: blade loading, cl: tip clearance losses and (3) the external losses (df: disc friction, rec: tip recirculation losses) as a function of the specific speed ns. The main driver for the compressor stage losses are clearly identified as the internal aerodynamic losses.

The external losses are characterized by very high disc friction losses at low speeds i.e. at large tip radius but decrease rapidly with decreasing wheel diameter. Disc friction is driven by the tip radius and to a lower extent by the gap from the wheel to the impeller backface. The actions to reduce disc friction are limited.

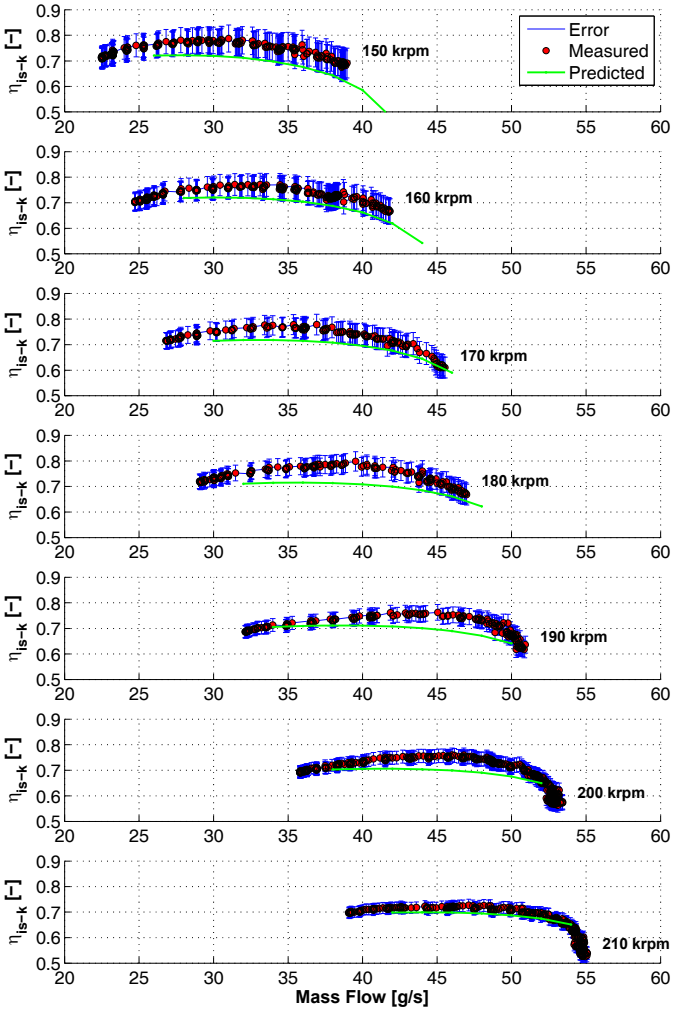

Figure 7: Measured and predicted internal isentropic efficiencies corresponding to the compressor map in Figure 6 for inlet conditions equivalent to an external air temperature of -12°C.

A closer analysis of the internal losses in Figure 9 reveals that the main driver for them is the skin friction. Except for very low rotational speeds all the internal losses increase with rotational speed. The cause is the amplitude of the relative speed at the leading edge and at the tip of the impeller, which increase with rotor speed. Skin friction is driven by the Re-numbers and by the relative surface roughness: for small-scale impellers the Re-number decreases (due to the lower tip with b_4) and the relative surface roughness increases, since the impeller is manufactured with the similar procedure as bigger ones. Both trends therefore penalize reduced scale impellers. Compressor stages operating in refrigerant fluids, however, do not suffer from low Re-number flows since the Re-numbers are generally high due to the low viscosity and increased density compared to air. Hence the main driver for the losses in small-scale impellers can be attributed to skin friction resulting from increased relative surface roughness. Recent work by Schiffmann (2013) has shown that small-scale compressor performance could be increased significantly by reducing the relative surface finish of the impeller by an additional polishing procedure.

Note that the tip clearance losses are relatively low although the impeller is small. This results from the appropriate choice of the journal bearings. The herringbone-grooved bearings are of rigid type, i.e. they allow to accurately position the rotor relative to the compressor housing. This allows to run at reduced relative tip clearances (in the order of 15-25% of the tip width b_4). Foil bearings, which are also very commonly used in small scale

turbomachinery, do not offer this possibility since their compliance yields inaccurate the rotor positions, hence larger tip clearances are needed in order to avoid impeller touchdown.

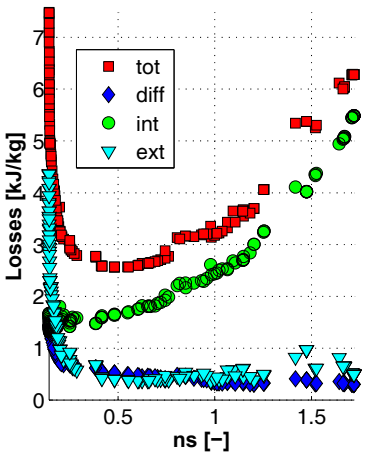

Figure 8: Split between internal, external and diffuser losses as a function of specific speed ns.

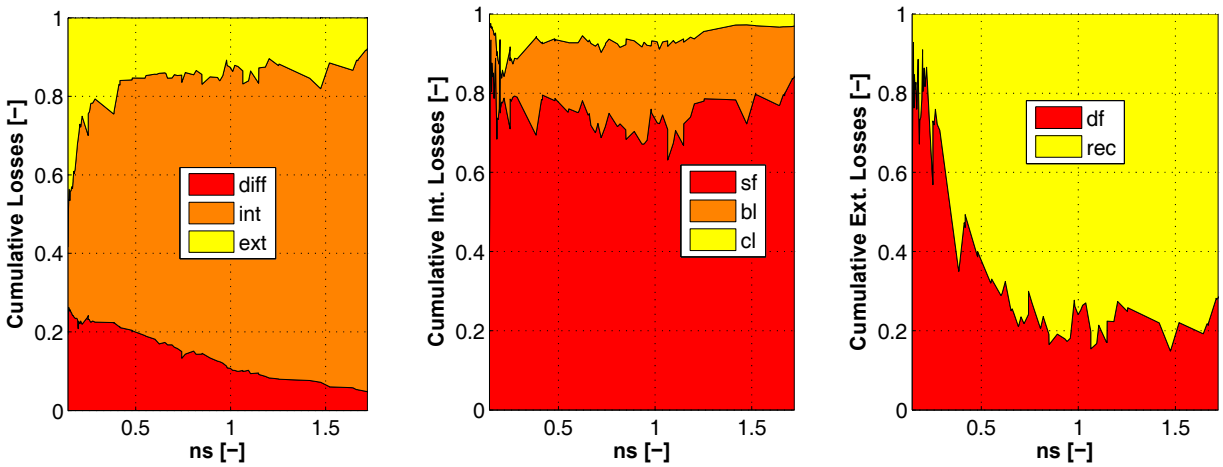

Figure 9: Split between (a) internal external and diffuser losses, (b) within the internal losses (sf: skin friction, bl: blade loading, cl: tip clearance losses, and (c) within the external losses (df: disc friction, rec: tip recirculation losses) as a function of the specific speed ns.

4. CONCLUSIONS AND OUTLOOK

A more rational use of the primary energy consumption for heating and cooling calls for the heat pump technology. The performance of today's systems is impaired by the presence of oil, which prevents the introduction of more efficient multi-stage cycles. Oil-free turbocompressors have been identified as a promising technology to increase the performance of heat pumps.

A test unit has allowed to prove the feasibility of such systems and demonstrates encouraging results. A proof-of-concept impeller with a tip diameter of 20 mm was tested at rotor speeds of up to 210 krpm reaching pressure ratios in excess of 3.3 and isentropic efficiencies of up to 79%. The system was directly driven by an electric motor and the shaft is supported on dynamic, gas-lubricated bearings, hence yielding a completely oil-free solution. The unit was tested in R134a.

NOMENCLATURE

b	Tip width	[mm]
β	Blade angle	[deg]
ns	specific speed	[-]
r	Radius	[mm]
η	Isentropic efficiency	[-]
Π	Pressure ratio	[-]
T	Temperature	[°C]
P	Pressure	[MPa]
COP	Coefficient of performance	
OP	Operation point	

REFERENCES

Burer, M., Favrat, D., Tanaka, K., Yamada, K., 2003, Multicriteria optimisation of a district heating cogeneration plant integrating a Solid Oxyde Fuel Cell-Gas Turbine combined cycle, heat pumps and chillers. *Energy, 28*(6), 497-518.

Demierre, J., Henchoz, S., Favrat, D., 2012, Prototype of a thermally driven heat pump based on integrated Organic Rankine Cycles (ORC). *Energy, 41*(1), 10-17.

Eschmann, M., 2008, *Monitoring von Klein-Waermepumpen mittels Normpruefungen 2008*: Swiss Federal Institute for Energy.

Favrat, D., Marechal, F., Epelly, O., 2008, The challenge of introducing an exergy indicator in a local law on energy. *Energy, 33*(2), 130-136.

Favrat, D., Nidegger, E., Reymond, D., Courtin, G., 1997, Comparison between a single-stage and a two-stage air to water domestic heat pump with one variable speed compressor. *IIR Conference on heat pump systems, energy efficiency and global warming, Linz, Austria*.

IEA., 2007, *Renewables for Heating and Cooling*: International Energy Agency.

Lund, J.W., 1968, Calculation of Stiffness and Damping Properties of Gas Bearings. *Journal of Lubrication Technology, 90*(4), 783-803.

Pan, C.H.T., 1964, *Spectral Analysis of Gas bearing systems for Stability Studies*: MTI-Report.

Schiffmann, J., 2013, Integrated Design and Multi-Objective Optimization of a Single Stage Heat-Pump Turbocompressor. ASME-Paper DETC2013-12180.

Schiffmann, J., Favrat, D., 2009, Experimental Investigation of a Direct Driven Radial Compressor for Domestic Heat Pumps. *International Journal of Refrigeration, 32*(8), 1918-1928.

Schiffmann, J., Favrat, D., 2010a, Design, experimental investigation and multi-objective optimization of a small-scale radial compressor for heat pump applications. *Energy, 35*(1), 436-450.

Schiffmann, J., Favrat, D., 2010b, The effect of real gas on the properties of Herringbone Grooved Journal Bearings. *Tribology International, 43*(9), 1602-1614.

Schiffmann, J., Favrat, D., 2010c, Integrated Design and Optimization of Gas Bearing Supported Rotors. *ASME Journal of Mechanical Design, 132*(5), 051007.

Youbi-Idrissi, M., Bonjour, J., Marvillet, C., Meunier, F., 2003, Impact of refrigerant-oil solubility on an evaporator performances working with R407c. *International Journal of Refrigeration, 26*(3), 284-292.

Zehnder, M., 2004, *Efficient Air-Water Heat Pumps for High Temperature Lift Residential Heating, including Oil Migration Aspects.* (PhD), Ecole Polytechnique Federale de Lausanne, Lausanne, Switzerland.

Zuercher, O., Thome, J. R., Favrat, D., 1998, Intube Flow Boiling of R-407C and R-407C/Oil Mixtures. Part I: Microfin Tube, . *HVAC/R Research ASHRAE, 4*(4), 347-372.